PROCEEDINGS OF THE SOCIETY FOR EXPERIMENTAL BIOLOGY AND MEDICINE 180, 174–184 (1985)

Impaired Organic Ion Transport in Proximal Tubules of Rats with Heymann Nephritis (42161)

E. K. PARK,* SUK KI HONG,‡ JAMES GOLDINGER,‡ GIUSEPPE ANDRES,*,† AND BERNICE NOBLE*,†

*Departments of *Microbiology, †Pathology, and ‡Physiology, School of Medicine, State University of New York, Buffalo, New York 14214*

Abstract. Organic ion transport across the basolateral membrane of proximal tubules was measured by means of the tissue slice technique in each of the four different stages of Heymann nephritis. Impairment of both organic anion and cation transport was detected early in Stage 2, and became more severe in Stage 3 of Heymann nephritis. The decreased transport function was associated with extensive damage to proximal tubule cells, including loss of brush border microvilli and basal infoldings. Despite these abnormalities of structure and function, oxygen consumption of proximal tubule cells remained essentially normal. Partial recovery of organic cation transport was noted late in Heymann nephritis (Stage 4). Recovery of the cation transport function was associated with a partial restoration of brush border microvilli and basal infoldings to proximal tubule cells. However, organic anion transport remained depressed throughout the entire course of disease. Impairment of organic ion transport in rats with Heymann nephritis appeared to result from damage to basolateral membrane transport elements rather than general deterioration of the metabolic machinery of proximal tubule cells. Decreased organic cation transport appeared to be the consequence of a reduction in the number of carrier sites, a phenomenon that could have resulted from decreased membrane surface area. However, the depression of organic anion transport was associated with decreased substrate affinity of the anion carrier, indicating that qualitative, rather than quantitative changes, were primarily responsible for that defect. Specific antibody-mediated damage to the anion transport elements in basolateral membranes of proximal tubules is postulated to occur in Heymann nephritis.

Immunization of some strains of rat with an extract prepared from rat kidney cortex produces an autoimmune disease known as Heymann nephritis (1, 2). Autoantibodies in the sera of rats with Heymann nephritis react *in vitro* with an antigen that is present in large amounts in the brush border of proximal tubules (3), and has also been demonstrated to be associated with epithelial cells of the glomerular capillary wall (4). Subepithelial granular immune deposits found in glomeruli of rats with Heymann nephritis appear to be formed by a reaction *in situ* of circulating autoantibodies with the epithelial cell antigen (5). As a consequence of increased permeability, resulting from the membranous lesion in glomeruli, circulating anti-brush border antibodies gain access to the proximal tubule lumen (6). The deposition of specific antibodies on the brush border membrane produces dramatic changes in proximal tubule histology (6, 7).

In several previous reports of kidney pathophysiology in Heymann nephritis (8–10), attention has been focused on the prominent glomerular lesion without serious consideration of the possible contribution of proximal tubule damage to overall kidney dysfunction. In another rat model of immunologically mediated interstitial nephritis, Wedeen *et al.* (11) studied the effect of antitubular basement membrane (TBM) and antibrush border antibodies on *p*-aminohippurate (PAH) transport and concluded that anti-TBM antibodies were associated with decreased uptake of PAH while anti-brush border antibodies were associated with decreased luminal PAH secretion *in vitro* and *in vivo*. Although antibodies to TBM and brush border were deposited *in vivo* simultaneously, no histological abnormalities were noted in proximal tubules. Therefore, that model of interstitial nephritis differed significantly from Heymann nephritis. Furthermore, in that

0037-9727/85 $1.50

study measurements were not made of parameters, such as oxidative metabolism and Na–K-ATPase activity, which are known to influence the active transport of PAH.

We have shown that the natural history of Heymann nephritis can be divided into four distinct stages with respect to immunopathology of proximal tubules (6). The delineation of discrete stages in the course of Heymann nephritis provides a rigorous basis for the correlation of kidney pathophysiology with proximal tubule immunopathology. The experiments described in this report were undertaken to assess the impact of proximal tubule injury on organic ion transport functions. Specific organic anion and cation transport functions were measured in each of the stages of Heymann nephritis by means of the tissue slice technique of Cross and Taggart (12). Collapse of the proximal tubule lumen in the kidney tissue slice precludes measuring transport properties of the brush border membrane; the uptake of organic ions by tissue slices is generally presumed, therefore, to reflect primarily activities of the basolateral membrane (13–15). Oxygen consumption of the slice, Na–K-ATPase activity, and tissue distribution of water were also analyzed, in order to detect possible alterations in cell metabolism that could affect organic ion transport by the basolateral membrane.

Methods. *Animals.* Female LEW rats, weighing 125 g, (Charles River Breeding Laboratories, Wilmington, Mass.) were immunized with Fx1A and adjuvant (see below) to produce Heymann nephritis. Others received injections of adjuvant alone. For study as completely normal controls, female LEW rats ages 3–4, 5–6, and 8–9 months were also obtained from the same company.

Antigen preparation. Frozen rat kidneys were purchased from Pel-Freeze Biologicals (Rogers, Ark.). The antigen fraction used for immunization, Fx1A, was prepared according to the method described by Edgington *et al.* (16).

Immunization protocols: Heymann nephritis. Rats were immunized in the hind footpads with 0.3 ml of an emulsion containing 10.0 mg of Fx1A, 0.5 mg of *Mycobacterium butyricum* (Difco Laboratories, Detroit, Mich.), 0.15 ml of saline, and 0.15 ml of complete Freund's adjuvant (Difco Laboratories, Detroit, Mich.). Twenty-eight days later, a second identical injection was administered in the front feet. Animals which developed Heymann nephritis exhibited significant proteinuria (>50 mg/24 hr) within 6 to 8 weeks of the initial immunization. Others, that failed to develop proteinuria despite immunization with Fx1A, were designated "nonresponders" (17).

Controls. Two groups of rats served as controls. One group was not immunized at all. Rats in that group were studied at different ages corresponding to the different stages of Heymann nephritis. Data obtained from those age-matched normal controls have been previously published (18) and are included here for comparison and reference. Rats in the second group received injections in the footpads consisting of 0.15 ml of saline, 0.15 ml of complete Freund's adjuvant, and 0.5 mg of *Mycobacterium butyricum.* Twenty-eight days later, an identical injection was given in the front feet. Rats in the adjuvant-treated control group were studied at times after immunization corresponding to the different stages of Heymann nephritis.

Plan of the experiments. Kidneys for tissue slice experiments were obtained from rats in each of the four stages of Heymann nephritis and from normal rats, age matched to each stage of Heymann nephritis. Nonresponders were studied at a time after immunization corresponding to Stage 3 of Heymann nephritis. In addition, rats immunized with adjuvant alone were studied. Those rats were killed 2 and 6 weeks after the second administration of adjuvant. When tissue slice experiments were performed, samples of kidney tissue were also obtained for examination by immunofluorescence and electron microscopy to permit an unequivocal identification of the stage of disease represented by each individual studied by the tissue slice technique.

Determination of the stages of Heymann nephritis. To monitor the course of Heymann nephritis, serum and urine samples were collected and analyzed weekly (6). Anti-brush border antibody titers were measured by means of indirect immunofluorescence tests. Urinary protein concentration was determined with the biuret test.

The following criteria, which have been

described previously (6), were used to distinguish the stages of Heymann nephritis.

Stage 1: Low, but increasing titers of circulating antibodies to brush border of proximal tubules. Weak granular immune deposits in glomerular basement membrane, no immune deposits in brush border of proximal tubules, normal proximal tubule morphology, no proteinuria. Rats in Stage 1 were approximately 3.5 months old.

Stage 2: High titers of circulating anti-brush border antibodies. Heavy granular immune deposits in glomerular basement membrane, heavy deposits of immunoglobulin in brush border of proximal tubule, damaged proximal tubule epithelium, proteinuria of 1- to 6-weeks' duration. Rats in Stage 2 were approximately 4–5 months old when studied.

Stage 3: Gradual decline in titers of anti-brush border antibodies. Heavy granular to ribbon-like immune deposits in glomerular basement membrane, weak or absent immune deposits in brush border, immune deposits along tubular basement membrane, damaged proximal tubule epithelium, proteinuria of 6- to 12-weeks' duration. Rats in Stage 3 were approximately 6–7 months old when studied.

Stage 4: Titers of circulating anti-brush border antibodies low or undetectable. Heavy ribbon-like deposits in glomerular basement membrane, no deposits in brush border and tubular basement membrane, substantial regeneration of proximal tubule epithelium, proteinuria of more than 12 weeks' duration. Rats in Stage 4 were 8–9 months old.

Nonresponders: Pattern of anti-brush antibody production resembling that seen in Heymann nephritis (17). Moderate accumulation of granular immune deposits in glomerular basement membrane. Normal protein excretion at all times and normal proximal tubule morphology.

Immunofluorescence tests. Kidney tissue samples for direct immunofluorescence tests were obtained and frozen when kidney slices were prepared for function tests. Indirect immunofluorescence tests to measure anti-brush border titers were performed on acetone-fixed frozen sections of normal rat kidneys. Details of the procedures used for direct and indirect immunofluorescence tests in our laboratory have been published elsewhere (6). FITC-conjugated antisera to rat immunoglobulins were purchased from Cappel Laboratories, Cochranville, Pennsylvania.

Histopathology. To evaluate tubule morphology in detail and to confirm that the natural history of Heymann nephritis in these experiments was identical to that described previously (6), several rats ($n = 3$) in each of the experimental groups were killed especially for study by light and electron microscopy. To achieve optimal fixation and preservation of the morphology of proximal tubules, the left kidney was fixed *in situ* by perfusion with 1% glutaraldehyde in modified Tyrode's buffer (19). Some pieces were embedded in paraffin, cut to 4-μm thickness, stained with hematoxylin–eosin, and examined with the light microscope. Other pieces of each kidney were postfixed in 1% osmium tetroxide, embedded in Epon–Araldite and prepared, by staining with lead hydroxide and uranyl acetate, for examination with the electron microscope (Siemens 101).

Slice experiments. Thin slices of the renal cortex (0.4–0.5 mm) were cut by hand and the slice uptake of *p*-aminohippurate (a representative organic anion) and tetraethyl-ammonium (TEA; a representative organic cation) were determined by a method described previously in detail (18). Briefly, the slices (150 mg wet wt) were incubated, unless stated otherwise, for 60 min in a modified Cross–Taggart medium (25°C) containing 7.5×10^{-5} *M* PAH or 1.0×10^{-5} *M* TEA and trace amounts of the respective ^{14}C-labeled organic ion (New England Nuclear, Boston, or Amersham, Arlington Heights, Ill.) under an oxygen atmosphere. After the incubation period, the concentrations of radiolabeled compounds in the tissue and incubation media were determined by liquid scintillation spectrometry. Detailed procedures for retreatment of slices as well as for quench correction are also described elsewhere (18). The uptake data were expressed as the slice-to-medium concentration ratio (S/M), defined as the disintegrations per minute (DPM) per gram wet tissue divided by the DPM per milliliter of incubation medium.

The S/M inulin ratio, as a measure of the

extracellular fluid space of the slice, was similarly determined by incubating the slice in the presence of [*carboxyl*-^{14}C]inulin (New England Nuclear) (18). The tissue water content was determined from the difference in weight before and after drying at 95°C for 24 hr (18).

To determine kinetic parameters of active organic ion transport, the total and passive uptakes of each ion during a 15-min incubation at 25°C were measured separately, and the difference was taken as active uptake. Previous studies conducted in our laboratory indicated that a 15-min incubation satisfies requirements needed to measure initial velocity (20). The total uptake was measured by incubating slices in an oxygenated medium containing various concentrations of PAH (50, 100, 200, 400, 800, and 1,600 μM) or TEA (20, 40, 80, 160, 320, and 640 μM). For the determination of passive transport, the slices were preincubated for 60 min under nitrogen atmosphere in a medium containing 0.1 mM each of 2,4 dinitrophenol (DNP) and iodoacetamide (IAA), and were then transferred for a 15-min incubation to the same medium containing various concentrations of PAH or TEA (see above).

The efflux of organic ions from renal cortical slices was determined by a modification of the technique used by Farah *et al.* (21). The slices were preloaded with the test compound for 60 min at 25°C. After preincubation, the tissues were rinsed briefly and then transferred at 1-min intervals through a series of 15-ml beakers that contained 3.0 ml of fresh Cross–Taggart medium (25°C). The quantity of compound collected from each runout chamber after exposure of the tissue plus the amount of compound that remained in the tissue after the experiment was used to construct the efflux curves and to calculate the rate constants.

The oxygen consumption of slices was measured with a Yellow Springs Instrument Company Model 53 oxygen monitor which employed a Clark-type electrode, as described earlier (18).

Na–K-ATPase activity. The Na–K-ATPase activity was determined in a crude homogenate of renal cortex, as described elsewhere (18, 22). The amount of inorganic phosphate liberated in the presence (total ATPase) and absence (Mg-ATPase) of KCl was determined. The difference was attributed to Na–K-ATPase. The concentrations of inorganic phosphate and tissue protein were analyzed by the method of Fiske and SubbaRow (23) and Bradford (24), respectively.

Statistics. A minimum of seven rats was used to obtain each mean value reported here. The data were analyzed statistically using Student's t test, either paired or unpaired, depending on experimental design.

Results. *Unimmunized rats.* An age dependency was observed in the magnitude of both PAH and TEA transport (S/M) by proximal tubules, as we have reported elsewhere (18) (Fig. 1). PAH transport decreased and TEA transport increased with age. Oxygen consumption and Na–K-ATPase activity did not change with age (Fig. 2).

Rats immunized with adjuvant alone. Two weeks after the second adjuvant immunization, corresponding to Stage 1 of Heymann nephritis, PAH transport was found to be 30% lower than in unimmunized rats of the same age ($P < 0.01$, Fig. 1). Na–K-ATPase was similarly reduced ($P < 0.001$, Fig. 2). Within 1 month, corresponding to Stage 2 of Heymann nephritis, both functions had returned to normal. Other parameters, including oxygen consumption, TEA transport, kidney size, and tissue water content were unaffected by immunization with adjuvant (Table I). Immunization with adjuvant alone did not produce detectable changes of kidney morphology.

Nonresponders. Nonresponders were indistinguishable from unimmunized rats of the same age with respect to all parameters studied (Table 1, Figs. 1 and 2). Tubules appeared completely normal, although glomeruli contained granular immune deposits of moderate intensity, as has been reported (26).

Rats with Heymann nephritis. Stage 1: Although TEA transport and oxygen consumption remained normal, PAH transport and Na–K-ATPase activity decreased to the same extent observed in rats given adjuvant alone (Figs. 1 and 2). Tissue water content, inulin space, and the ratio of kidney weight to body weight were not significantly different from age-matched or adjuvant-treated con-

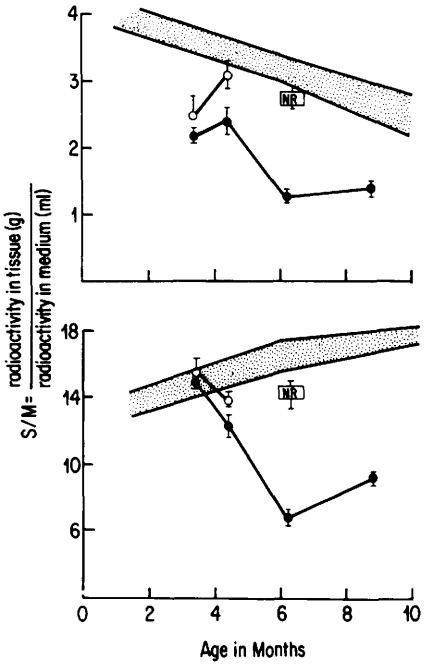

FIG. 1. PAH transport (upper graph) and TEA transport (lower graph) in different stages of Heymann nephritis. Mean values (±1 SE) obtained with normal unimmunized rats at different ages (covering a range corresponding to the natural history of Heymann nephritis) are from Park *et al.* (18) and are indicated by the shaded areas. Animals with Heymann nephritis (HN), indicated by ●, were in Stage 1 at 3.5 months, Stage 2 at 4.5 months, Stage 3 at 6 months, and Stage 4 at 9 months of age. Animals immunized with adjuvant alone (○) were studied at 3.5 months of age, 2 weeks after the second and final adjuvant administration, and at 4.5 months of age. Nonresponders, NR, were studied at an age corresponding to Stage 3. The error line indicates ±1 SE. The concentrations of PAH and TEA in the medium were 75 and 10 μM, respectively.

trols. No unusual aspect of tubule cell morphology was noted. Immunofluorescence microscopy confirmed that immune deposits were limited to glomeruli, as has been previously described (6).

Stage 2: A reduction of PAH and TEA transport functions was observed (PAH, 25% reduction, $P < 0.02$; TEA, 25% reduction, $P < 0.01$, Fig. 1). Na–K-ATPase was decreased (35% reduction, $P < 0.001$), although oxygen consumption was maintained at normal rates (Fig. 2). Tissue water content, extracellular water content, and kidney weight remained normal (Table I). As has been shown before (6), heavy deposits of immunoglobulins were present along the luminal membrane of the proximal tubules, with focal, weaker deposits at the basal side of tubule cells. Microvilli were damaged and missing from many tubule cells and basolateral infoldings were also decreased in some tubule cells. No abnormalities of mitochondria were noted.

Stage 3: Severe deficits in PAH and TEA transport were detected in Stage 3 of Heymann nephritis (PAH, 60% reduction, $P < 0.001$; TEA, 60% reduction, $P < 0.001$, Fig. 1). On the other hand, neither Na–K-ATPase activity nor oxygen consumption differed significantly from corresponding values in either control group. An increase in weight of the kidney appeared to result from

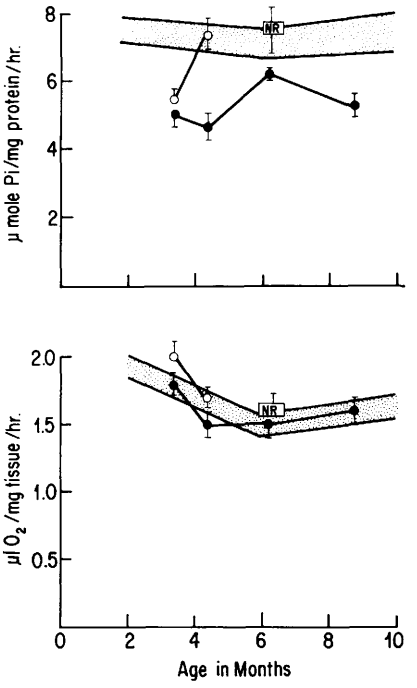

FIG. 2. Na–K-ATPase activity (upper graph) and O_2 consumption (lower graph) in different stages of Heymann nephritis. Mean values (±1 SE) obtained with normal unimmunized rats at different ages are from Park *et al.* (18) and are indicated by the shaded areas. Stage 1 of Heymann nephritis (HN, ●) = 3.5 months, Stage 2 = 4.5 months, Stage 3 = 6 months, Stage 4 = 9 months. Animals immunized with adjuvant alone (○) were studied 2 and 6 weeks after the final adjuvant injection, at ages corresponding to Stages 1 and 2 of Heymann nephritis. Nonresponders, NR, were studied at 6 months of age, corresponding to Stage 3.

TABLE I. ANTIBODY TITER, PROTEIN EXCRETION, AND KIDNEY WATER CONTENT IN DIFFERENT STAGES OF HEYMANN NEPHRITIS

Group	*n*	Approximate age (months)	Urinary protein excretion (mg/24 hr)	Anti-brush border titer (log_2)	Kidney wt / Body wt (%)	Kidney H_2O content (%)	Inulin space (S/M)
Unimmunized**	20	4.5	12.4 ± 0.4	—	1.0 ± 0.1	75.7 ± 0.3	0.31 ± 0.01
Adjuvant only**	31	4.5	9.6 ± 0.8	—	0.9 ± 0.1	77.4 ± 0.6	0.35 ± 0.01
Heymann nephritis							
Stage 1	15	3.5	15.3 ± 2.3	6.1 ± 0.5	0.9 ± 0.1	77.0 ± 0.4	0.34 ± 0.01
Stage 2	15	4.5	81.4 ± 7.4*	6.8 ± 0.3	1.0 ± 0.1	77.9 ± 0.5	0.36 ± 0.01
Stage 3	14	6.0	196.4 ± 20.7*	3.4 ± 0.4	1.3 ± 0.1*	81.3 ± 0.1*	0.41 ± 0.01*
Stage 4	16	8.5	280.3 ± 41.1*	1.3 ± 0.5	1.4 ± 0.1*	81.5 ± 0.7*	0.45 ± 0.02*
Nonresponders	15	6.0	15.6 ± 2.3	4.8 ± 0.5	0.9 ± 0.1	78.4 ± 0.4	0.34 ± 0.01

* Significantly different from normal, $P < 0.01$.
** In these groups, mean values of all parameters did not vary with age from 3.5 to 8.5 months.

an increase in total kidney tissue water content. Measurements of the inulin space (S/M) showed that the water had accumulated, at least partially, in extracellular sites (Table I).

By direct immunofluorescence tests, only weak focal deposits of immunoglobulins were seen on the luminal aspect of the proximal tubule cells. Granular immune deposits were detected along the tubular basement membrane as well as in glomeruli (Fig. 3). The most severe damage to proximal tubules, previously described to occur in Stage 3 of Heymann nephritis (6) was also noted in Stage 3 in these experiments. The cells of the proximal tubules were greatly flattened, showing extensive loss of microvilli, greatly decreased basolateral infoldings and thickened tubule basement membranes with electron dense deposits (Fig. 4). Despite these dramatic

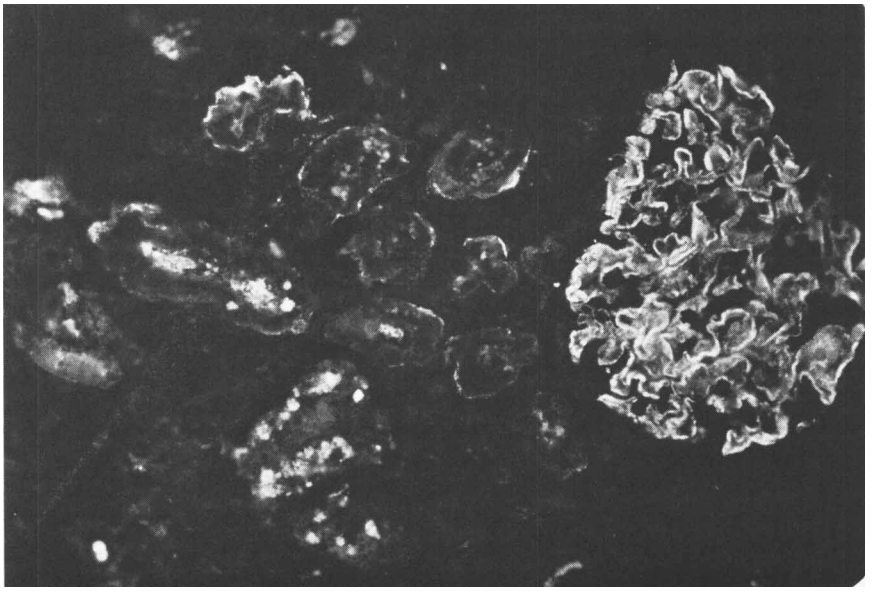

FIG. 3. Frozen kidney section from a rat in Stage 3 of Heymann nephritis, stained by the direct immunofluorescence technique for rat IgG. Granular deposits can be seen along the glomerular capillary wall and at the base of many proximal tubules. There is little staining of the brush border (×250).

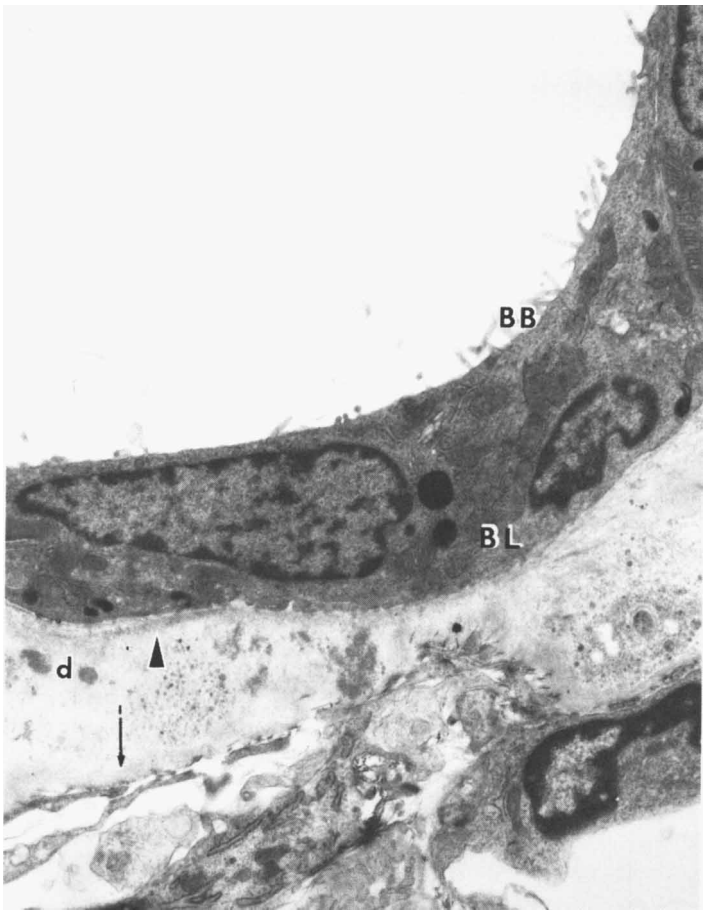

FIG. 4. Electron micrograph of a proximal tubule from a rat in Stage 3 of Heymann nephritis. Microvilli are largely absent from the brush border (BB) and the basolateral membrane (BL) is devoid of invaginations. The original tubular basement membrane (arrow) lies far below the plasma membrane and is wrinkled and thickened. Dense deposits (d) lie above the original tubular basement membrane. A new basement membrane appears to be forming just below the plasma membrane of the cell (arrowhead; ×5000).

changes in proximal tubule cell morphology, no changes in mitochondria were noted in this stage of Heymann nephritis.

Transport kinetics and organic ion efflux were also studied in Stage 3 in which the transport deficit was greatest. The Michaelis–Menten constant (K_m) for active PAH transport was more than twice the normal value (0.62 mM vs 0.25 mM), whereas the maximum reaction velocity (V_{max}) of the reaction was unchanged compared to normal (Fig. 5). For active TEA transport, K_m was not altered in Heymann nephritis, but V_{max} was substantially reduced (58.8 nmole/g tissue/min vs 33.3 nmole/g tissue/min, Fig. 6). The efflux rate constant for preaccumulated PAH was normal in rats with Heymann nephritis (0.074 ± 0.001 vs 0.072, ± 0.001, $n = 3$), as was the TEA efflux rate constant (0.025 ± 0.003 vs. 0.030 ± 0.002, $n = 3$).

Stage 4: A small but significant recovery of TEA transport function, compared to Stage 3 of Heymann nephritis, was observed (35% recovery, $P < 0.001$, Fig. 1). However, no improvement in PAH transport was observed (Fig. 1). An increased concentration of extracellular tissue water persisted (Table I). In the final stage of Heymann nephritis, immune

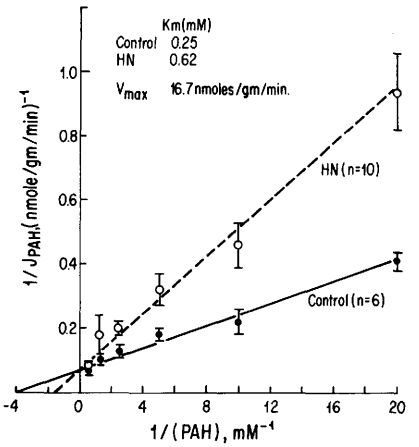

FIG. 5. Lineweaver–Burke analysis of initial rate of active transport of PAH (J) in normal rats (●) and rats in Stage 3 of Heymann nephritis (○). See Methods for the determination of active transport component. Numerical figures in parentheses indicate the number of rats.

deposits, detectable by immunofluorescence tests, were limited to glomeruli. Recovery of a nearly normal morphology was observed in many proximal tubules (Fig. 7), with restoration of microvilli and basal infoldings.

Discussion. In rats with Heymann nephritis, antibody-mediated damage to the proximal tubule epithelium was associated with substantial impairment of the transport of organic ions across the basolateral membrane. Oxygen consumption and mitochondrial morphology remained essentially normal throughout the course of Heymann nephritis.

Impairment of organic ion transport functions in Heymann nephritis did not seem to be attributable to either systemic or local effects of proteinuria and/or other aspects of the nephrotic syndrome. Proximal tubule transport of organic ions has been found to be normal in rats with moderate chronic serum sickness (18) that exhibit proteinuria, hypoalbuminemia, and hyperlipidemia comparable to Heymann nephritis (25, 26). Significant defects in PAH and TEA transport, detected in rats with severe chronic serum sickness (18), result from a general deterioration of the metabolic machinery of proximal tubule cell metabolism rather than direct injury to the plasma membrane. Furthermore, the presence, in glomeruli alone, of immune deposits containing anti-brush border antibody did not appear to affect transport functions of the proximal tubules, as nonresponders were indistinguishable from controls.

Although PAH transport is functionally linked to Na–K-ATPase activity (22), the marked inhibition of PAH uptake observed in Stage 3 was not accompanied by a corresponding inhibition of Na–K-ATPase. A modest inhibition of PAH uptake observed early in Heymann nephritis was associated with 30–35% inhibition of Na–K-ATPase. However, studies by Spencer *et al.* (22) indicate that PAH uptake in the slice is not significantly affected unless Na–K-ATPase activity is inhibited more than 50%. Therefore, the small inhibition of PAH uptake observed during Stages 1 and 2 of Heymann nephritis is probably not linked to the modest inhibition of Na–K-ATPase. The fact that both the tissue oxygen consumption and water content remained normal during Stages 1 and 2 also indicates that the *in situ* operation of the Na–K exchange pump mediated by this enzyme was well preserved.

To investigate the possibility that immunological injury produced alterations in the specific carrier proteins, kinetic aspects of organic ion transport were studied. In Heymann nephritis, the number of anion carrier molecules, or their turnover rate (as reflected by V_{max}), was not altered. However, the affin-

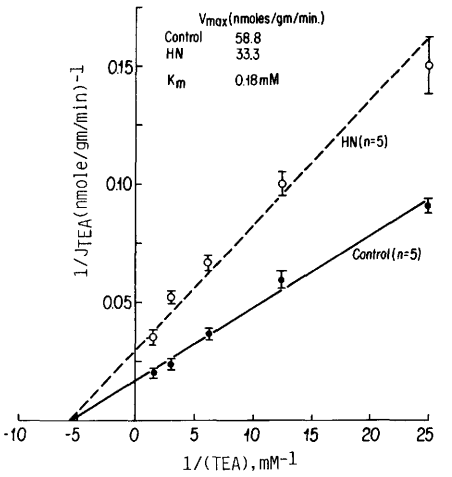

FIG. 6. Lineweaver–Burke analysis of initial rate of active transport of TEA (J) in normal rats (●) and rats in Stage 3 of Heymann nephritis (○). See legend to Fig. 5 for other details.

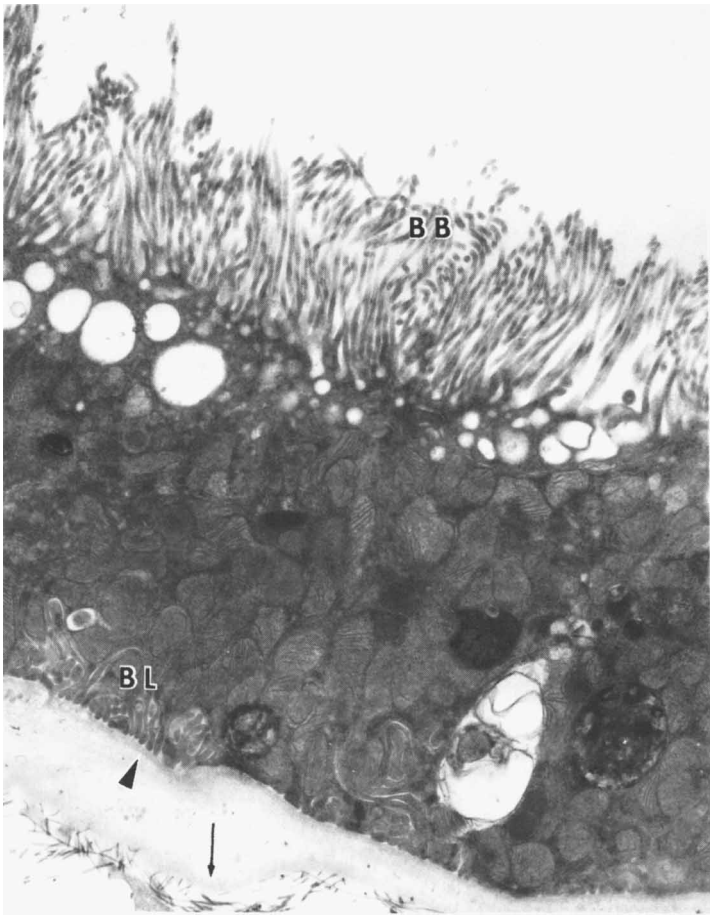

FIG. 7. Electron micrograph of a proximal tubule from a rat in Stage 4 of Heymann nephritis. The microvilli of the brush border (BB) have a normal appearance. Invaginations are present in the basolateral membrane (BL). The original basement membrane is indicated by an arrow. Dense deposits are no longer visible between the old basement membrane and the newly formed basement membrane which lies closely apposed to the basal infoldings (×5000).

ity of that carrier (as reflected by apparent K_m) for the substrate, PAH, was approximately 50% lower in sick rats than in age-matched controls. In contrast, the affinity of the cation carrier for TEA remained unaltered, although the number of cation carriers, or their turnover rate, was reduced considerably (about 50%) in Heymann nephritis. These changes, in cation carrier number and anion carrier substrate affinity, may explain the depression in basolateral membrane transport activity that we have observed in Heymann nephritis.

At present, it is only possible to speculate about the molecular mechanisms by which the carrier elements for organic ion transport may be compromised in Heymann nephritis. Loss of basolateral invaginations, which greatly decreases membrane surface area, would be expected to lead to equal reduction of both anion and cation transport carrier sites. The observation of a reduction in the number of only TEA carriers indicates that the anion and cation carrier elements are not similarly distributed in the basolateral membrane and suggests that anion carriers may be located in sites protected from the loss of membrane surface area that occurs in Heymann nephritis. In that respect, it is interesting to note that gp 330, the antigen implicated

in glomerular pathology of Heymann nephritis, has also been described to be heavily concentrated in clathrin-coated invaginations at the base of the microvilli of the luminal membrane (27). The PAH carrier might also be similarly sequestered in the basolateral membrane.

The partial recovery of cation transport in Stage 4 is consistent with the hypothesis that cation transport depression results from decreased basolateral membrane surface area. Recovery of function is similar in magnitude (about 35%) to the semiquantitative estimate that has been made of the extent of recovery of normal morphology (6). However, reduction of V_{max} for cation transport, and not anion transport, could also be explained by an entirely different mechanism. If the loss of basolateral membrane surface area, as a consequence of immune injury, was limited to S_1 and S_3 segments only, significant reduction in the number of only cation carrier elements would be expected, as PAH transport occurs primarily in S_2 segments (30). We believe that possibility to be unlikely, as morphological studies performed to date have not revealed differential susceptibility of individual proximal tubule segments to antibody-mediated injury. More precise and detailed morphometric analysis of proximal tubule damage is required to clarify this point.

Defects in PAH transport function in Heymann nephritis appear to be attributable to qualitative, rather than quantitative changes in anion carrier elements, as indicated by an increase in K_m. Such qualitative alterations could have resulted from a specific immunological reaction between the anion carrier and autoantibodies produced as a consequence of immunization with Fx1A. Although antibodies reacting specifically with basolateral membrane antigens have not previously been implicated in the immunopathology of Heymann nephritis, there is considerable circumstantial evidence for their existence. Fine, granular deposits of immunoglobulin, detectable at the basal portion of many proximal tubule cells in Stage 1 of Heymann nephritis become more prominent as the disease progresses and are the most striking feature of proximal tubule immunofluorescence in Stage 3 (6). The subepithelial location of the deposits and their strict limitation to proximal tubules suggest strongly that a specific immune reaction accounts for their formation (28). It is most likely that those deposits form at the base of proximal tubule cells by a mechanism similar to the reaction *in situ* that leads to the subepithelial accumulation of deposits along the glomerular basement membrane in Heymann nephritis. Antibodies responsible for the peritubular deposits could be identical with, or closely related to, those deposited in glomeruli and on the brush border. On the other hand, since the complex antigenic composition of tubule cell membranes may result in the production of autoantibodies with a variety of specificities (29), those deposited along the basolateral membrane may be completely unrelated to the anti-brush border antibodies. Alternatively, it is possible that the close physical association of the anion carrier with another membrane antigen, against which autoantibodies are directed, results in steric hindrance of PAH transport.

Injection of adjuvant alone was followed by a moderate, transient inhibition of the transport of PAH, but not TEA. This inhibitory effect of adjuvant treatment is the most probable explanation for the reduction in PAH transport detected in Stage 1 of Heymann nephritis and in mild chronic serum sickness (18). The implication is that adjuvant treatment may produce a direct effect on organic anion transport. It remains to be determined whether this effect on membrane function is limited to the kidney.

This investigation was supported by Grants AM26394, AI10334, and AM18918 of the National Institutes of Health. The authors thank Susan Alder and Pam Gigliotti for expert technical assistance and Dr. J. B. Van Liew and Dr. J. R. Brentjens for extremely valuable discussions.

1. Edgington TS, Glassock RJ, Dixon FJ. Autologous immune-complex pathogenesis of experimental allergic glomerulonephritis. Science **155**:1432–1434, 1967.
2. Heymann W, Hackel DB, Harwood S, Wilson SGF, Hunter JLP. Production of nephrotic syndrome in rats by Freund's adjuvants and rat kidney suspension. Proc Soc Exp Biol Med **100**:660–664, 1959.
3. Grupe WE, Kaplan MH. Demonstration of an antibody to proximal tubular antigen in the pathogenesis

of experimental autoimmune nephrosis in rats. J Lab Clin Med **74**:400–409, 1969.
4. Kerjaschki D, Farquhar MG. Immunocytochemical localization of the Heymann nephritis antigen (gp 330) in glomerular epithelial cells of normal Lewis rats. J Exp Med **157**:667–686, 1983.
5. Couser WG, Steinmuller DR, Stilmant MM, Salant DJ, Lowenstein LM. Experimental glomerulonephritis in the isolated perfused rat kidney. J Clin Invest **62**:1275–1287, 1978.
6. Mendrick D, Noble B, Brentjens J, Andres G. Antibody-mediated injury to proximal tubules in Heymann nephritis. Kidney Int **18**:328–343, 1980.
7. Noble B, Mendrick DL, Brentjens JR, Andres GA. Antibody-mediated injury to proximal tubules in the rat kidney induced by passive transfer of homologous anti-brush border serum. Clin Immunol Immunopathol **19**:289–301, 1981.
8. Allison MEM, Wilson CB, Gottschalk CW. Pathophysiology of experimental glomerulonephritis in rats. J Clin Invest **53**:1402–1423, 1974.
9. Bernard DB, Alexander EA, Couser WG, Levinsky NG. Renal sodium retention during volume expansion in experimental nephrotic syndrome. Kidney Int **14**:478–486, 1978.
10. Ichikawa I, Hoyer JR, Seiler MW, Brenner BM. Mechanism of glomerulotubular balance in the setting of heterogeneous glomerular injury. J Clin Invest **69**:185–198, 1982.
11. Wedeen RP, Batuman V, Sobel H. Effect of antitubular basement membrane and brush border antibodies on p-hippurate transport in kidney. Nephron **29**:258–264, 1981.
12. Cross RJ, Taggart JV. Renal tubular transport: Accumulation of p-aminohippurate by rabbit kidney slices. Amer J Physiol **161**:181–190, 1950.
13. Arthus MF, Bergeron M, Scriver CR. Topology of membrane exposure in the renal cortex slice studies of glutathione and maltose cleavage. Biochim Biophys Acta **693**:371–376, 1982.
14. Kinter WB, Wong MD. Peritubular membrane transport of PAH into proximal cells in Necturus kidney slices. Amer J Physiol **227**:50–57, 1974.
15. Burg MB, Orloff J. p-Aminohippurate uptake and exchange by separated renal tubules. Amer J Physiol **217**:1064–1068, 1969.
16. Edgington TS, Glassock RJ, Dixon FJ. Autologous immune complex nephritis induced with renal tubular antigen. I. Identification and isolation of the pathogenetic antigen. J Exp Med **127**:555–572, 1968.
17. Noble B, Van Liew JB, Andres GA, Brentjens JR. Factors influencing susceptibility of Lew rats to Heymann nephritis. Clin Immunol Immunopathol **30**:241–254, 1984.
18. Park EK, Andres G, Hong SK, Noble B. Proximal tubule function in chronic serum sickness glomerulonephritis of rats. Proc Soc Exp Biol Med **178**:105–113, 1985.
19. Maunsbach A. The influence of different fixatives and fixation methods on the ultrastructure of rat kidney proximal tubules cells. 2. Effects of varying osmolality, ionic strength, buffer system and fixative concentration of glutaraldehyde solutions. J Ultrastruct Res **15**:283–309, 1966.
20. Gerencser GA, Hong SK. Roles of sodium and potassium ions in p-aminohippurate transport in rabbit kidney slices. Biochim Biophys Acta **406**: 108–119, 1975.
21. Farah A, Frazer M, Stoffel M. Studies on the runout of p-aminohippurate from renal slices. Amer J Physiol **139**:120–127, 1963.
22. Spencer AM, Sack J, Hong SK. Relationship between PAH transport and Na-K-ATPase activity in the rabbit kidney. Amer J Physiol **236**:F126–F130, 1979.
23. Fiske CH, SubbaRow Y. The colorimetric determination of phosphorous. J Biol Chem **66**:375–400, 1925.
24. Bradford MM. A rapid and sensitive method for the quantitation of microgram quantities of protein utilizing the principle of protein-dye binding. Anal Biochem **72**:248–254, 1976.
25. Van Liew JB, Brentjens JR, Noble B. Relationship of kidney function to immunopathology in chronic serum sickness of rats. Kidney Int **24**:160–169, 1983.
26. Van Liew J, Noble B, Brentjens JR. Absence of sodium and water retention in rats with severe proteinuria. Nephron **40**:476–481, 1985.
27. Kerjaschki D, Noronha-Blob, Sacktor B, Farquhar MG. Microdomains of distinctive glycoprotein composition in the kidney proximal tubule brush border. J Cell Biol **9**:1505–1513, 1984.
28. Woodhall PB, Tisher CC, Simonton CA, Robinson RR. Relationship between para-aminohippurate secretion and cellular morphology in rabbit proximal tubules. J Clin Invest **61**:1320–1329, 1978.
29. Miettinen A, Tornroth T, Ekblom P, Virtanen I, Linder E. Nephritogenic and non-nephritogenic epithelial antigens in autoimmune and passive Heymann nephritis. Lab Invest **50**:435–446, 1984.
30. Noble B, Brentjens JR, Andres GA. Autoimmune kidney diseases. In: Rose NR, Mackay IR, eds. The Autoimmune Disease. New York, Academic Press, in press.

Received February 25, 1985. P.S.E.B.M. 1985, Vol. 180.
Accepted May 14, 1985.